molecular pharmaceutics

ARTICLE

pubs.acs.org/molecularpharmaceutics

Polymer Swelling, Drug Mobilization and Drug Recrystallization in Hydrating Solid Dispersion Tablets Studied by Multinuclear NMR Microimaging and Spectroscopy

Carina Dahlberg,[†,‡] Sergey V. Dvinskikh,[†] Michael Schuleit,[§] and István Furó*[,†]

[†]Division of Physical Chemistry and Industrial NMR Centre, Department of Chemistry, Royal Institute of Technology, SE-100 44 Stockholm, Sweden

[§]Forum 1, Pharmaceutical & Analytical Development, Novartis Pharma AG, Novartis Campus, CH 4056 Basel, Switzerland

[‡]YKI, Institute for Surface Chemistry, Box 5607, SE-114 86 Stockholm, Sweden

Supporting Information

ABSTRACT: Despite the advantages offered by solid dispersions, the marketed products based on this technology are few. The most frequent concern is the stability of the amorphous drug. The state of the drug in solid dispersions is, in general, poorly characterized as the number of characterization techniques available to monitor nanometer-sized drug particles embedded in a matrix are limited. Here we present a combination of localized NMR spectroscopic and NMR imaging techniques which allow *in situ* monitoring of the state of the drug during tablet disintegration and dissolution. ^{19}F NMR relaxation is shown to be sensitive to both the crystalline/amorphous state and the size of the model nanoparticles made of the drug substance flutamide. The time course of drug mobilization and recrystallization is detected with spatial resolution within swelling solid dispersion tablets. Comparing results from spatially resolved ^{19}F, ^{2}H and ^{1}H NMR experiments, recrystallization is related to its enabling factors such as local hydration level and local mobility of the polymer matrix. The initially amorphous drug may recrystallize either by nanoparticle coalescence or by ripening of crystalline grains.

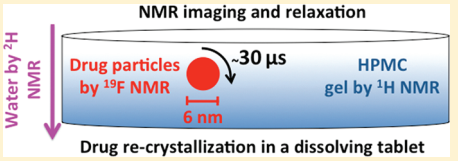

KEYWORDS: recrystallization kinetics, amorphous drug nanoparticles, particle size, in situ monitoring, NMR imaging, hydroxypropyl methylcellulose HPMC

INTRODUCTION

A clear majority of the new lead candidates in the pharmaceutical pipeline are classified as poorly water-soluble. To increase their bioavailability, the industry seeks new formulation strategies.[1] One such strategy is to solubilize and disperse drugs in the liquid phase by surface active agents such as lipids. Another strategy attempts to modify dissolution kinetics by dispersing the drug as small solid particles, which increases the dissolution rate via increased surface-to-volume ratio which increases solvent access. Moreover, small particles with high curvature may shift the solid form of drug to a state of higher free energy that may increase solubility and the rate of dissolution. Having the drug in amorphous instead of a crystalline phase can also improve dissolution properties.[2−5] In a broader perspective, nanotechnology-based approaches for particle size reduction are novel but promising toward increasing improved dissolution characteristics. One interesting approach is tablets or capsules consisting of nanoparticles prepared from dried nanosuspensions.[6]

Solid dispersions, in which the drug in its supposedly amorphous form is incorporated in a solid matrix typically made of hydrophilic polymer,[7−11] are favored over most other methods as concerning oral delivery of hydrophobic drugs. However, the success has been hampered by their instability. The amorphous state with its higher internal energy and more molecular motion is inherently thermodynamically unstable and is prone to recrystallize either during storage or at initial exposure to liquid environment.[12,13] If that happens, bioavailability may decrease.

Techniques which can be used to produce solid dispersions are melting/solidification, melt extrusion, or solvent evaporation.[7] Whichever path is selected, the outcome—the size and amorphous/crystalline state of the particles—remains uncertain and must be characterized in order to develop rational strategies to optimize the created formulations. However, experimental techniques that can obtain information about the state of nanometer-sized drug particles embedded in a matrix are scarce; hence, the state of solid dispersions is, in general, poorly characterized. The most commonly used methods available for examining particle size and amorphous/crystalline state have severe limitations when applied to solid dispersions pressed into tablets.[4,11] Powder X-ray diffraction (pXRD)[14] and differential scanning calorimetry (DSC)[2,15,16] are neither spatially resolved nor capable of distinguishing between the drug being molecularly dispersed or being distributed as small amorphous grains or small (below a few nanometers) crystalline grains. Optical and chemical characterization of amorphous or crystalline drug particles of micrometer size can be performed by scanning electron microscopy (SEM)[17]

Received: February 1, 2011
Accepted: June 22, 2011
Revised: June 17, 2011
Published: June 22, 2011

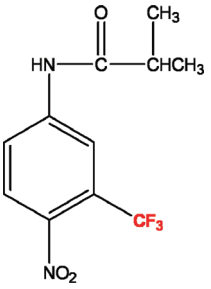

Figure 1. The molecular structure of flutamide.

or by micro-Raman spectroscopy.[17,18] However, particles in the nanometer size range are too small to be detected. To date, there are only very few studies where one could obtain explicit and verifiable information about the state of drugs in solid dispersions where the drug component lacked the usual attributes of large crystalline grains such as peaks in a pXRD pattern. Those investigations were performed with transmission electron microscopy (TEM)[19,20] and nanothermal analysis (nano-TA).[21] Both techniques observe surface behavior and are therefore invasive (that is, require sufficiently thin slices) as concerning monitoring the particle size in the bulk of a tablet (or during tablet dissolution). Though not spatially resolved, pXRD coupled with the computation of pair distribution functions[22−24] shows promise for distinguishing between solid dispersions of amorphous particles and solid drug/matrix solutions (that is, molecularly distributed drug) systems. Magic angle spinning (MAS) solid-state NMR spectroscopy also can distinguish between amorphous and crystalline states of small drug particles,[25−29] and may also be able to detect whether or not one has a solid solution.

Here we present a combination of localized nuclear magnetic resonance (NMR) spectroscopy and NMR imaging techniques[30,31] which allow *in situ* investigation of the drug under these particular conditions. These techniques are often used, though typically for observing the water and water dynamics in pharmaceutical formulations.[32−46] As we demonstrate below, the state of the drug can also be monitored during tablet disintegration and dissolution. In particular, we observe drug recrystallization from the initial state identified as amorphous nanoparticle. The approach we present may be useful in a broader perspective of material characterization.

MATERIAL AND METHODS

Sample Preparation. In preparing the solid dispersions, the carrier hydroxypropyl methylcellulose (HPMC, Dow Chemical, USA), the model drug flutamide (Sigma-Aldrich), whose structure is shown in Figure 1, and the solvents ethanol (Alco Suisse), acetone (Shell) and distilled water were used. The solubility of flutamide in water is 30 mg/L (ca. 110 μM, determined by UV/vis spectrophotometry). D_2O (99.9 atom % D, Sigma-Aldrich) was used as penetrant solvent.

Solid dispersions with a flutamide concentration of 15 wt % were prepared by rotoevaporation according to Dahlberg et al.[47] and milled to a particle size distribution of <200 μm. As a proof of concept, solid dispersions with this fairly low drug content, assumed (and also verified below) to be homogeneously distributed, were used. Physical mixture with 15 wt % milled flutamide (milled in the same manner as the solid dispersions) in HPMC

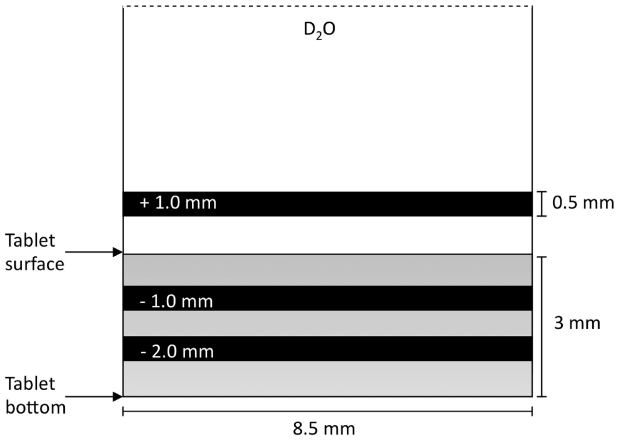

Figure 2. Schematic image of the positioning of the three different slices deep within (at −1 and −2 mm measured from the original tablet surface) and above (at +1 mm) the tablet, from which signal is acquired.

(used as received) was also prepared by thorough mixing in jars. All powders were stored at 8 °C in a closed container.

For the ^{19}F longitudinal relaxation time measurements in bulk, "gel samples" were prepared by thoroughly mixing 150 mg of sample powder with 0.5 mL of D_2O.

For the recrystallization kinetics experiments with spatial resolution, 150 mg tablets (diameter 8.5 mm, height 3 mm) were pressed directly in the sample tubes by using two pistons and a laboratory press (Spectac, England). The homemade sample tubes similar to those used by us earlier,[48] restricting the swelling to one dimension, were produced from Teflon for the ^{1}H and ^{2}H experiments and from Capron (PA-6) for the ^{19}F experiments. Tablet swelling and transformation was initiated by layering 2 mL of D_2O on the tablet top (marking time = 0 for the presented data). Here we note that we have previously demonstrated the high reproducibility of our tablet preparation and NMR/MRI protocols.[48]

NMR and MRI Experiments. All experiments were performed on a Bruker Avance III 500 spectrometer using a Bruker Diff 30 probe equipped with commercial ^{1}H and ^{2}H radiofrequency (rf) inserts and a homemade ^{19}F rf insert, respectively.

All imaging experiments were set up to provide one-dimensional images along the tablet axis direction that coincided with the direction of the magnetic field B_0. In this arrangement, water was layered on the top of the tablet resulting in vertical swelling along the tablet axis. Constant time imaging (CTI)[49,50] was implemented as previously described.[48] The experimental parameters are provided in detail as Supporting Information. As has been discussed previously,[43,48,51] under the selected experimental conditions and at lower hydration levels (such as in the original tablet volume and up to ca. 70−80% water content) the ^{1}H signal intensity reflects the local polymer mobility as imprinted in the ^{1}H transverse relaxation time. At higher water content, such as in the gel layer above the original tablet surface, the ^{1}H signal intensity reflects the local polymer concentration.

In the ^{19}F localized spectroscopy experiments different slices, approximately 0.5 mm thick, were explored by Gaussian selective pulses with 10% truncation level and a half-height of approximately 40 kHz. The slices presented here (see Figure 2) were positioned 2 mm below, 1 mm below and 1 mm above the original tablet surface. We note that the results (see Figure 3) obtained in two different tablets (see also below) show a close overlap which

indicates good reproducibility. The apparent ^{19}F transverse relaxation rate R_2^* was estimated from the line width Δ (as $R_2^* = \pi\Delta$) by fitting single Lorentzian lineshapes to the spectra recorded for the different slices. Note that some spectra had clearly two components (one somewhat narrower and another one broader) and therefore our R_2^* data are to be considered as rough estimates. Nevertheless, these data span over the full range of swelling and therefore provide a comprehensive illustration. The ^{19}F tranverse relaxation rate, R_2, was also measured in bulk samples in a spatially unresolved manner by fitting single exponentials to data obtained by conventional spin−echo experiments.

The ^{19}F longitudinal relaxation time T_1 was measured in each slice at certain time intervals by a modified inversion recovery experiment consisting of a shaped Gaussian inversion pulse and a nonselective detection pulse. By applying every second shaped pulse very far off resonance and subtracting the data from every second scan, the signal from the selected slice was retained and the signal from everywhere else canceled. By varying the delay between the inversion pulse and the detection pulse, the signal intensity showed an apparent exponential decay to zero at large waiting times. By fitting a single exponential to the decay points (see examples in Supporting Information, Figure S1), T_1 was obtained with an estimated precision of ca. 3%. CTI is, in principle, also capable of providing the spatial distribution of T_1. We found, however, that the results were forbiddingly sensitive to rf inhomogeneity which is a consequence of the large sensitivity of the CTI signal to the flip angle.[52] The ^{19}F longitudinal relaxation time, T_1, was also measured in bulk samples in a spatially unresolved manner by fitting single exponentials to data obtained by conventional inversion recovery experiments.

Powder X-ray Diffraction (pXRD). The analyses were performed using a Ni-filter and Cu Kα radiation, at a voltage of 45 kV and a current of 35 mA (XRD, PANalytical X'Pert PRO, The Netherlands). The scanning rate was 0.1° s^{-1} over the range of 5−60°.

RESULTS AND DISCUSSION

First of all, we would like to stress that, with samples prepared as above and with water concentrations explored,[48] the NMR signal obtained at different resonance frequencies (that of ^{1}H, ^{19}F and ^{2}H) is selective as concerning molecular species: the ^{1}H signal arises mainly from the HPMC matrix (with minor contributions from ^{1}H in the drug and from ^{1}H spins transferred by proton exchange to water), the ^{2}H signal arises from the water and the ^{19}F signal arises from the drug, flutamide. In particular, ^{19}F NMR can selectively monitor the molecular state of the drug component in the presence of an overwhelming amount of water and polymer matrix.[53]

The results below can be grouped into three parts, closely connected but necessarily discussed separately. The first two parts form the background for the last part. The first part concerns the manner by which NMR can be used to establish and monitor the crystalline state of the model drug flutamide. In the second part, we consider the initial state of the flutamide that is embedded in the HPMC matrix. Finally and based on our spatially resolved NMR parameters, we discuss the time course of drug mobilization and recrystallization and the factors influencing those within the swelling solid dispersion tablet.

Recrystallization of Flutamide in Bulk. We rely on two techniques to detect the crystalline state of flutamide.[54] Of these, powder X-ray diffraction (pXRD) is a widely used routine method. The other investigated parameter, the longitudinal relaxation time T_1, cannot, in contrast to pXRD, be used for deducing the atomic arrangement in crystals but, as has been exemplified,[53,55−63] is responsive to the crystalline form of a particular substance. T_1 is sensitive to the crystalline state, because the intermolecular potentials in a lattice provide lattice-specific local molecular dynamics on the time scale of the inverse Larmor frequency (here, on the order of 10^{-10}−10^{-9} s). Besides, the NMR line width may also carry information about the crystalline state although this latter parameter is a more complex function of molecular dynamics (and can often be measured less accurately).

Flutamide as received consisted of needle-like crystals.[54] If dispersed in water, those crystals reoriented in the sample tube when placed in the magnetic field (as shown by the presence of a clear dipole modulation pattern of the line shape[64]). Since T_1 in crystals is often orientation dependent,[65,66] we milled our flutamide (to small round grains) for the measurements below in order to avoid orientation effects that would be absent in solid dispersions. We followed the behavior of three materials after having them mixed with water: flutamide, the physical mixture (PM) of flutamide and hydroxypropyl methylcellulose (HPMC), and the solid dispersion (SD) of flutamide in HPMC matrix. In the latter two cases, mixing with water resulted in gels.

The initial state of flutamide in the dry SD (identical to "SD 5 min" in Figure 4) is not crystalline as testified by the lack of discrete scattering peaks and has a T_1 value that is less than half of that recorded for dry flutamide or flutamide in the PM (see Figure 5 at $t = 0$). At the same point, the transverse relaxation time $T_2 = 1/R_2$ obtained by spin echo was approximately 55 μs. The shorter T_1 value and the fact that we are far from the extreme narrowing regime ($T_1 \gg T_2$) indicate that the molecular mobility of flutamide is significantly higher in the SD than in the bulk crystals; recrystallization suppresses mobility.[55,59] T_1 is dominated by short-range effects which are expected to be similar in small (∼nm) and large (≫nm) crystals. Plausibly, the drug in the SD either is in the form of amorphous grains or is molecularly distributed in the matrix.

A few hours after mixing the SD powders with water, pXRD peaks characteristic of flutamide crystals appear above the noise threshold (see Figure 4), clearly indicating recrystallization of the drug in the forming gel. The longitudinal relaxation time, T_1, was monitored over time for the different powders immersed into water; the data obtained are shown in Figure 5. During the first hour, the transverse relaxation time T_2 obtained by spin echo remained in the range 55−70 μs (width comparable to experimental accuracy), which indicates, on the other hand, that T_2 is dominated by slow motions. Pure flutamide and the PM behave similarly and show T_1 being insensitive to mixing with water (one should note that the increased motional freedom of >μm crystalline grains, now in water, has no effect on T_1 because T_1 is solely influenced by motions with short correlation times, on the order of 10^{-10}−10^{-9} s). The increase of T_1 in SD clearly indicates that flutamide involved in a HPMC gel recrystallizes, on the time scale of hours, after having been placed in an aqueous environment. At long times, the ^{19}F T_1 for the SD is similar to that of the PM and the pure flutamide.

The Initial State of Flutamide in the Solid Dispersion. As discussed above, the initial state of the drug in a (dry) solid dispersion is, in general, poorly characterized. From the lack of sharp XRD peaks, it is clear that there are no large (≫10 nm) crystalline particles present. From the ^{19}F longitudinal relaxation,

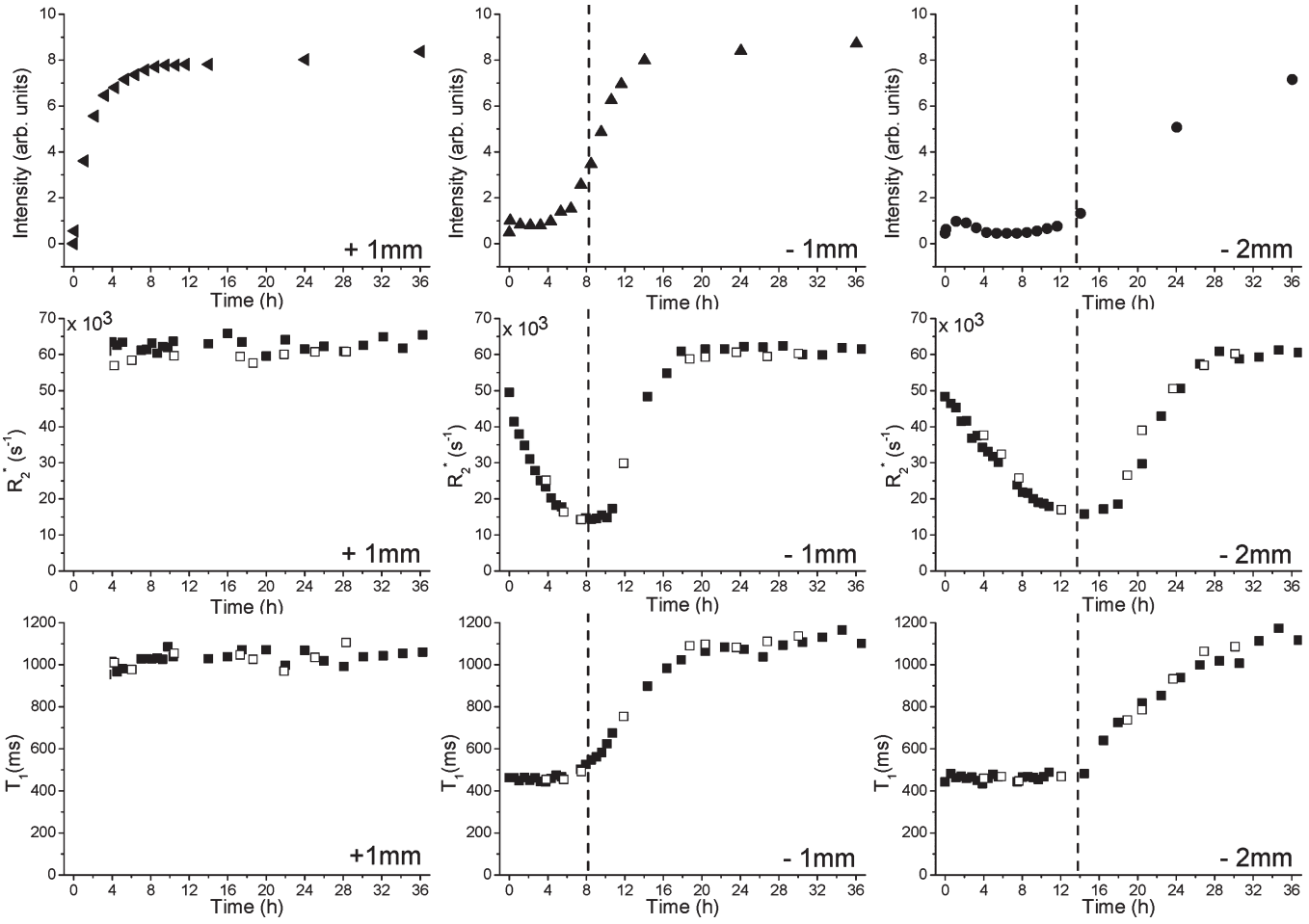

Figure 3. The variation of ^{1}H polymer signal intensity (a, upper row), the apparent ^{19}F transverse relaxation rate R_2^* estimated from the line width (b, middle row) and the ^{19}F longitudinal relaxation time (c, bottom row) in the different slices, see Figure 2, over time. The dashed line is marking the position of t_{min}, see text. Filled and unfilled symbols represent measurements in two different tablets.

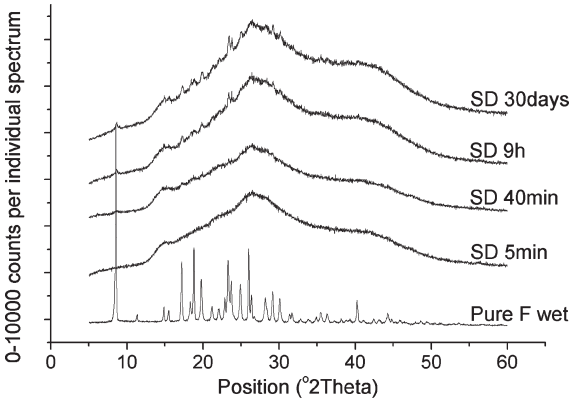

Figure 4. X-ray powder diffraction pattern for wet flutamide and flutamide/HPMC solid dispersion (SD) "gels". The time of contact between powder and water is increasing from below.

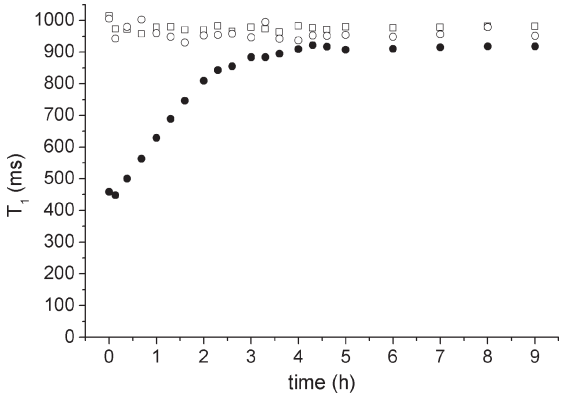

Figure 5. T_1 change in bulk over time for powders (flutamide, □; physical mixture, PM, ○; and solid dispersion, SD, ●) mixed with water. The time of first contact between the powder and the water is set to $t = 0$.

we know that the drug lacks short-range crystalline order which indicates that the drug either is in the form of amorphous grains or is molecularly distributed in the HPMC matrix. Below, we shall explore the measured ^{19}F relaxation rates (see Figure 3) to gather some additional information.

Spin relaxation[67,68] depends on the random motion of particles (which, at this point, can be either grains or individual molecules). If spin relaxation arises, as here, from intramolecular spin interactions, it is the rotational diffusion that is the underlying dynamical mode. For a particle, the rotational correlation

time, τ_c, can be expressed via the Debye−Stokes−Einstein equation as

$$\tau_c = \frac{4\pi}{3k_B T}\eta {r_H}^3 \quad (1)$$

where k_B is Boltzmann's constant, T is the temperature, r_H is the hydrodynamic radius of the diffusing entity and η is the viscosity of the surrounding medium. (Note that at low levels of hydration and with a structural heterogeneity on the microscopic level, microviscosity and (macroscopic) viscosity do not necessarily coincide.[69]) For HPMC, macroscopic viscosity data have been measured at accessibly low polymer concentrations (in dense gels like ours, measuring viscosity is difficult by common measuring techniques such as U-tube viscometers[70]). Hence, for the same kind of HPMC we use, the viscosity has been reported to be 100 mPa s in aqueous solutions at the highest explored HPMC concentration of 15 wt % at 20 °C.[71] Any reasonable, linear or polynomial on the logarithmic scale, extrapolation puts viscosity to 5 Pa > η > 1 Pa at ca. 70 wt % HPMC content.

At low hydration (that corresponds in Figure 3 to early ($<t_{min}$) times and at positions −1 and −2 mm within the tablet), the transverse relaxation rate has been measured by spin echo experiments in bulk samples (see above) to be in the range $R_2 = 1/T_2 \approx (14-18) \times 10^3\ s^{-1}$. In contrast, at low hydration the inhomogeneous decay rate R_2^* deduced from the line width is up to $50 \times 10^3\ s^{-1}$. The difference can be ascribed static dipolar broadening that is not refocused in spin echo experiments.[72] Even if bond rotation is typically fast enough for CF_3 groups in organic substances to reduce the $^{19}F-^{19}F$ dipole−dipole coupling to a residual value,[64,73] the static dipole−dipole broadening is apparently not zero, which explains the $R_2 < R_2^*$ situation. On the other hand, at t_{min} in Figure 3 we experience $R_2 \approx R_2^*$, which thereby indicates the lack of static dipole−dipole at that level of hydration (in addition, this finding also shows that other line broadening effects such as magnetic field inhomogeneity are not significant in setting the value of R_2^*). The difference at any time between transverse and longitudinal relaxation rates (see Figures 3b and 3c) indicates that flutamide ^{19}F spin relaxation is far from the extreme narrowing regime. As the matrix becomes hydrated, mobility increases,[35,48,74] which provides some reorientational freedom for the flutamide particles (which, at this point, can be assumed to be grains or individual molecules). This leads to motional averaging of the residual coupling and, ultimately, to a line width that is dominated by transverse relaxation. A similar situation is often encountered in other materials, and the model we use here (that is, for accounting for transverse relaxation dominated by slower motions averaging a residual coupling) is termed as the two-step model.[75−78] The motion responsible for averaging the residual coupling must still be slow ($\omega_0\tau_c \gg 1$) as shown, indeed, by $R_1 \ll R_2$ for ^{19}F in the whole investigated region. Hence, at t_{min} the transverse relaxation rate R_2 for ^{19}F becomes directly proportional to the correlation time τ_c.

The main relaxation mechanism for ^{19}F nuclei is via the dipole−dipole coupling.[67,68] In the case of a CF_3 group, the dominant contribution originates from the $^{19}F-^{19}F$ couplings within the group. In general, the dipolar relaxation of three equivalent spin-1/2 nuclei is a rather complex process[73,79,80] and is further complicated by the fact that the dynamics is contributed to by motional modes both fast (in our case, rotational diffusion around the C−C bond) and slow (rotational diffusion of the flutamide particles). However, the analysis can be simplified just like other cases[75−78] (i) by assuming that the bond rotation mode is sufficiently fast[73] not to contribute to the observed transverse relaxation and (ii) by making use of the residual dipole−dipole coupling (χ_{DD}^{res} = 15.8 kHz[64]) that is left unaveraged by the bond rotation and is available from static dipole−dipole splitting data. If the rotational diffusion of the particles is sufficiently slow, one can then express the transverse relaxation rate[68] as

$$R_2(^{19}F) = \frac{1}{20}(2\pi\chi_{DD}^{res})^2\tau_c \quad (2)$$

We shall below exploit this relaxation for deducing the state of flutamide in the solid dispersion, both at low hydration and at t_{min}.

As water penetrates into the tablet, it softens up the HPMC network, which results in a decreasing microviscosity with increasing water content. Since flutamide solubility in water is very low, we do not expect that increasing water content *per se* changes the hydrophobic flutamide particles (such as particle breakup, which would increase thermodynamically unfavorable surface contact with water) that are embedded in the matrix. However, it permits the flutamide particles to tumble faster, which manifests itself, as discussed above, in a decrease of the ^{19}F line width because the tumbling averages the residual static dipole−dipole coupling until a minimum (t_{min} in Figure 3b) is reached. It is very important to note that the ^{19}F longitudinal relaxation is *constant* up to t_{min} (see Figure 3c) which indicates that the fast local motions and thereby the immediate molecular environment for flutamide are also constant. Hence, we find that the most plausible model that encompasses both of these observations is that the flutamide is in the form of amorphous grains and not in the form of molecular solution; the *overall tumbling* of the grains (reflected in the line width) responds to the increasing hydration and thereby the decreasing viscosity while the local molecular motions of the flutamide molecules (reflected in the longitudinal relaxation) *within* the grains remain virtually unchanged, at least up to t_{min}.

Note that the initial state of the tablet is not completely dry; from drying experiments, that initial water content is estimated to a few wt %. For comparison, at 8 h ($=t_{min}$) after the initiation of tablet hydration and swelling at 1 mm under the tablet surface the amount of added water can be estimated from the ^2H NMR signal intensity to approximately 25−30 wt %. Similar water content is obtained at t_{min} for the slice at 2 mm under the tablet surface. Our transverse relaxation data at t_{min} provide, via eq 2, that the rotational correlation time τ_c of grains is approximately 30 μs. By assuming that the viscosity at that level of hydration is η > 1 Pa, we obtain from eq 1 that the hydrodynamic radius of the flutamide grains must be <3 nm. This size limit is robust because the hydrodynamic radius obtained by this analysis depends on the third root of viscosity. To illustrate, even if we take the 100 mPa s viscosity obtained at a much higher water content (at 15 wt % HPMC), the particle size limit barely increases to <6.5 nm. As concerning lower size limit, the hydrodynamic radius of a single flutamide molecule is below 1 nm (see Figure 1). Hence, a correlation time τ_c in the order of 30 μs would require viscosities >30 Pa (unlikely, see above) to be able to account for our observations under the hypothesis of a molecular solution. In addition, we note that the rotational correlation times of *single molecular* spin labels with sizes similar to that of flutamide have been measured by ESR spectroscopy[74,81] in HPMC tablets with hydration levels similar to those here. Those rotational correlation

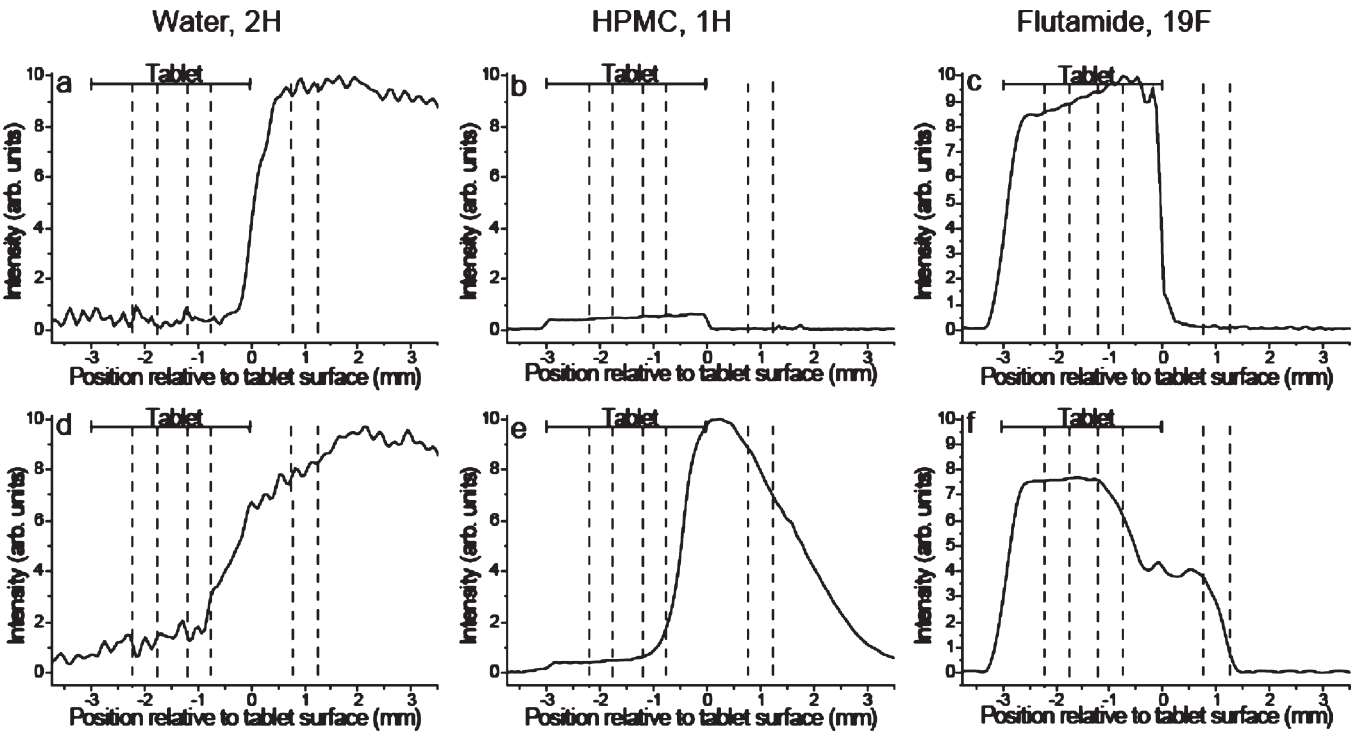

Figure 6. Example of one-dimensional CTI profiles of the water concentration (a/d), the concentration of mobile polymers (b/e) and the drug concentration (c/f) along the *z*-axis of the dissolving tablet (positions in the originally dry tablet are on the negative *x*-axis). Profile (a) is acquired directly after water addition, profiles (b, c) prior to water addition and profiles (d,e,f) 6 h after water addition. The dashed lines indicate the positions of the three selected slices.

times were found to be <100 ns, *more than 2 orders of magnitude faster* than the rotational correlation time obtained here for flutamide. Considering that $\tau_c \propto r_H^3$, that finding is consistent with the molecular radius of <1 nm setting, in those experiments, the correlation time for tumbling. This also excludes us having, at least at t_{min}, a solid solution of flutamide in the matrix.

Hence, we conclude here that the most probable initial state of the flutamide is amorphous grains of a few nm size. Below, we investigate how this initial state responds to increasing hydration and swelling.

Tablet Behavior and Drug Recrystallization Kinetics during Swelling. As we have established above, ^{19}F NMR relaxation is sensitive to the crystalline state of flutamide. We shall explore this finding below to map recrystallization within the SD tablet. Additionally, we connect recrystallization to its enabling factors such as local hydration level and local mobility of the polymer matrix. This is made possible by the isotope and chemical selectivity of NMR spectroscopy and NMR imaging; hence, ^{19}F NMR spectroscopy and NMR imaging will selectively report on the state and distribution of the drug, ^{1}H NMR imaging will provide information about tablet swelling and about the changes in local polymer mobility, and ^{2}H NMR imaging will measure water penetration into the tablet.

The qualitative features of tablet swelling are illustrated by the 1D profiles presented in Figure 6. The data presented in Figure 3 illustrate further other aspects of tablet evolution. The longitudinal relaxation time T_1 in Figure 3c reflects molecular dynamics in the 10^{-10}–10^{-9} s time scale. Since we are far from the extreme narrowing regime,[67,68] any *decrease* reflects *increasing* molecular mobility. The transverse relaxation rate R_2^*, as obtained directly from the line width, is sensitive to changes on a much broader time scale,[67,68] in our case from 10^{-3} to 10^{-10} s. Far from the extreme narrowing regime, the transverse relaxation reacts to changes in molecular mobility oppositely to longitudinal relaxation. Hence, a *decrease* in R_2^* (that is, an increase in the corresponding relaxation time) reflects *increasing* molecular mobility. This is the reason for plotting the transverse relaxation *rate* and the longitudinal relaxation *time* together in Figure 3.

We note that, to some extent, all profiles presented in Figure 6 are influenced by relaxation effects although this effect is small for the ^{19}F and ^{2}H images while dominant for the ^{1}H images. In other words, they do not solely report on local concentration but also on local molecular dynamics (for further details, see Supporting Information). At the expense of experimental time, these two effects can be separated. However, for our present purpose such composite images suffice (one can also note that slight additional distortions arise from the inhomogeneity of the radiofrequency field). They confirm the chain of following processes: water penetrates the tablet (^{2}H profiles), polymer chains in the hydrated regions become more mobile and the resulting water rich gel expands upward (^{1}H profiles), and the expanding gel carries the drug (^{19}F profiles). One can, in addition, see that in the initial state the drug is homogeneously distributed within the tablet. In contrast to the polymeric component whose transverse relaxation rate changes by several orders of magnitude during the course of hydration, R_2^* for the drug component is changing by less than a factor of 5 (see Figure 3). Hence, the ^{19}F intensities presented reflect less the changes in molecular mobility and more the local drug concentration. Comparing the ^{1}H and ^{19}F profiles, it is, nevertheless, clear the drug is "left behind" by the upward expanding and progressively weakening gel (in this context, note that the signal intensity that arises from dissolved flutamide is

below noise level because of the small aqueous solubility of flutamide[82]). Our analysis above led us to the suggestion that the flutamide is initially collected in grains that are in the size range of a few nanometers. Indeed, with such a structure the behavior observed here can be easily rationalized by the polymer gel reaching such a water content that the mesh size becomes comparable to and/or exceeds the particle size.

In the volume above the original tablet surface, the increase of ^{1}H intensity reflects the expansion of the polymer gel into that volume. In parallel, the concentration of water as reflected by the ^{2}H NMR intensity decreases above the tablet surface.[47] Although not shown specifically, at very long times (when the whole tablet is well hydrated and swollen up and is in part dissolved) the water (and polymer) signals reach the same values in all selected slices. In the slice above the surface of the originally dry tablet, the detected ^{19}F T_1 corresponds all the time to that of crystalline drug (Figure 3c). This is not surprising since it takes a few hours for the expanding polymer gel to reach that region and, as shown in Figure 4, this time is sufficient for recrystallization of the originally amorphous drug.

In contrast, the variation of spin-relaxation parameters in slices within the originally dry tablet is far more dramatic and nontrivial. There, early on in the dissolution process, R_2^* is decreasing while T_1 remains roughly constant. This can be, as discussed above, rationalized by recalling that R_2^* is sensitive, in contrast to T_1, to slower molecular dynamics. Hence, decreasing R_2^* signifies the increasing tumbling of the drug particles allowed by the increasingly hydrated and thereby less viscous gel. It takes time for water to diffuse deep into the tablet.[47] Hence, the observed variation in Figure 3 is slower and t_{min} is larger in the slice deeper inside the tablet than those in the shallower slice. At all points in the tablet the water content is continually increasing and thereby the viscosity is continually decreasing. Hence, the increase of R_2^* above t_{min} which indicates slower particle tumbling can only be explained by the increase of particle size above t_{min}. On the other hand, up to t_{min} the molecules within the grains do not exhibit a change in their molecular environment as indicated by the constant value of T_1.

The most remarkable observation is the close coincidence, in the different slices, of the times at which R_2^* reaches its minimum with the point where T_1 starts to increase. This indicates that the local onset of recrystallization (T_1) coincides with onset of growth of particles. While the most natural mechanism for the growth of grains is ripening mediated by flutamide that becomes dissolved in the penetrating water phase, the coincidence described above prompts us to speculate about an alternative molecular mechanism. As detailed above, increasing hydration increases the tumbling of the small initial flutamide grains; this must be equally valid for their translational diffusion. As the grains diffuse further and further, they can come into contact with each other with increasing frequency. Upon contact the grains may coalesce, and that may increase grain size, leading to slower tumbling and increasing R_2^*, but it can also *induce recrystallization* as signified by the increase of T_1. Recrystallization that proceeds by such a scenario is known to other areas such as the transformation of nanocrystalline anatase to rutile where the mechanism is termed interface nucleation.[83−85] The molecular explanation involves both motional freedom and molecular supply at the point of contact of amorphous grains which favors molecular rearrangement into a thermodynamically stable crystalline state. Further growth can progress by aggregation and/or ripening.[86−88] Further studies may help to distinguish between these possibilities.

CONCLUSIONS

Our results improve the understanding of pharmaceutical formulations in general and that of solid dispersions in particular in two directions. First, we demonstrate that NMR imaging, with support from a complementary technique (pXRD), is a highly capable tool for following the changes in the state of matter within swelling and dissolving pharmaceutical formulations. In particular, the highly relevant process of recrystallization can be assessed in detail and with a spatial resolution that is probably not currently available by other methods. The same method can plausibly be adapted in a straightforward manner for studying the behavior of any other drug that contains fluorine. Moreover, the same method could be applicable to model drugs that do not contain fluorine assuming that one uses ^{13}C localized spectroscopy in samples prepared by in ^{13}C-enriched drugs.

Further, we present convincing evidence that in our solid dispersion the initial state of the drug is small (3−4 nm) amorphous grains distributed homogeneously in the polymer matrix. Upon hydration the motional freedom of drug nanoparticles increases within the increasingly mobile polymer matrix. We detect that the onset of recrystallization coincides with the start of the increase of the grain size. This leads us to speculate that interface nucleation instead of ripening may be the underlying mechanism for the recrystallization. Further studies of the effect of drug properties, drug−carrier interactions, carrier stabilization and manufacturing process are highly desirable to improve our understanding of solid dispersions.

ASSOCIATED CONTENT

Supporting Information. Additional experimental details, table of acquisition parameters for the different CTI experiments, and figure depicting examples of data and fits for obtaining T_1 under different conditions. This material is available free of charge via the Internet at http://pubs.acs.org.

AUTHOR INFORMATION

Corresponding Author

*Royal Institute of Technology, Department of Chemistry, Physical Chemistry, Teknikringen 36, SE-100 44 Stockholm, Sweden. E-mail: furo@kth.se Tel: +46 8 7908592. Fax: +46 8 7908207.

ACKNOWLEDGMENT

This work has been supported by Novartis Pharma AG, the Swedish Research Council VR and Knut and Alice Wallenberg Foundation. We thank Anna Millqvist-Fureby for useful discussions.

REFERENCES

(1) Fahr, A.; Liu, X. Drug delivery strategies for poorly water-soluble drugs. *Expert Opin. Drug Delivery* **2007**, *4* (4), 403–416.

(2) Saleki-Gerhardt, A.; Zografi, G. Non-isothermal and isothermal crystallization of sucrose from the amorphous state. *Pharm. Res.* **1994**, *11* (8), 1166–1173.

(3) Hancock, B. C.; Zografi, G. Characteristics and significance of the amorphous state in pharmaceutical systems. *J. Pharm. Sci.* **1996**, *86* (1), 1–12.

(4) Yu, L. Amorphous pharmaceutical solids: preparation, characterization and stabilization. *Adv. Drug Delivery Rev.* **2001**, *48* (1), 27–42.

(5) Urbanetz, N. A.; Lippold, B. C. Solid dispersions of nimodipine and polyethylene glycol 2000: dissolution properties and physicochemical characterisation. *Eur. J. Pharm. Sci.* **2005**, *59* (1), 107–118.

(6) Chaubal, M. V.; Popescu, C. Conversion of nanosuspensions into dry powders by spray drying: A case study. *Pharm. Res.* **2008**, *25* (10), 2302–2308.

(7) Chiou, W. L.; Riegelman, S. Pharmaceutical applications of solid dispersion systems. *J. Pharm. Sci.* **1971**, *60* (9), 1281–1302.

(8) Serajuddin, A. T. M. Solid dispersion of poorly water-soluble drugs: Early promises, subsequent problems, and recent breakthroughs. *J. Pharm. Sci.* **1999**, *88* (10), 1058–1066.

(9) Leuner, C.; Dressman, J. Improving drug solubility for oral delivery using solid dispersions. *Eur. J. Pharm. Sci.* **2000**, *50* (1), 47–60.

(10) Vasconcelos, T.; Sarmento, B.; Costa, P. Solid dispersions as strategy to improve oral bioavailability of poor water soluble drugs. *Drug Discovery Today* **2007**, *12* (23−24), 1068–1075.

(11) Chow, K.; Tong, H. H. Y.; Lum, S.; Chow, A. H. L. Engineering of pharmaceutical materials: an industrial perspective. *J. Pharm. Sci.* **2008**, *97* (8), 2855–2877.

(12) Murphy, D.; Rodríguez-Cintrón, F.; Langevin, B.; Kelly, R. C.; Rodríguez-Hornedo, N. Solution-mediated phase transformation of anhydrous to dihydrate carbamazepine and the effect of lattice disorder. *Int. J. Pharm.* **2002**, *246* (1−2), 121–134.

(13) Greco, K.; Bogner, R. Crystallization of amorphous indomethacin during dissolution: Effect of processing and annealing. *Mol. Pharmaceutics* **2010**, *7* (5), 1406–1418.

(14) Ghebremeskel, A. N.; Vernavarapu, C.; Lodaya, M. Use of surfactants as plasticizers in preparing solid dispersions of poorly soluble API: Selection of polymer-surfactant combinations using solubility parameters and testing the processability. *Int. J. Pharm.* **2007**, *328* (2), 119–129.

(15) Bhugra, C.; Shmeis, R.; Krill, S. L.; Pikal, M. J. Different measures of molecular mobility: Comparison between calorimetric and thermally stimulated current relaxation times below T_g and correlation with dielectric relaxation times above T_g. *J. Pharm. Sci.* **2008**, *97* (10), 4498–4515.

(16) Andronis, V.; Yoshioka, M.; Zografi, G. Effects of sorbed water on the crystallization of indomethacin from the amorphous state. *J. Pharm. Sci.* **1997**, *86* (3), 346–351.

(17) Papageorgiou, G. Z.; Bikiaris, D.; Karavas, E.; Politis, S.; Docoslis, A.; Park, Y.; Stergiou, A.; Georgarakis, E. Effect of physical state and particle size distribution on dissolution enhancement of nimodipine/PEG solid dispersions prepared by melt mixing and solvent evaporation. *AAPS J.* **2006**, *8* (4), 623–631.

(18) Docoslis, A.; Huszarik, K. L.; Papageorgiou, G. Z.; Bikiaris, D.; Stergiou, A.; Georgarakis, E. Characterization of the distribution, polymorphism, and stability of nimodipine in its solid dispersions in polyethylene glycol by micro-Raman spectroscopy and powder X-ray diffraction. *AAPS J.* **2007**, *9* (3), 361–370.

(19) Karavas, E.; Georgarakis, E.; Sigalas, M. P.; Avgoustakis, K.; Bikiaris, D. Investigation of the release mechanism of a sparingly water-soluble drug from solid dispersions in hydrophilic carriers based on physical state of drug, particle size distribution and drug-polymer interactions. *Eur. J. Pharm. Sci.* **2007**, *66* (3), 334–347.

(20) Karavas, E.; Georgarakis, M.; Docoslis, A.; Bikiaris, D. Combining SEM, TEM, and micro-Raman techniques to differentiate between the amorphous molecular level dispersions and nanodispersions of a poorly water-soluble drug within a polymer matrix. *Int. J. Pharm.* **2007**, *340*, 76–83.

(21) Zhang, J.; Bunker, M.; Chen, X.; Parker, A. P.; Patel, N.; Roberts, C. J. Nanoscale thermal analysis of pharmaceutical solid dispersions. *Int. J. Pharm.* **2009**, *380*, 170–173.

(22) Newman, A.; Engers, D.; Bates, S.; Ivanisevic, I.; Kelly, R. C.; Zografi, G. Characterization of Amorphous API:Polymer Mixtures Using X-Ray Powder Diffraction. *J. Pharm. Sci.* **2008**, *97* (11), 4840–4856.

(23) Ivanisevic, I.; Bates, S.; Chen, P. Novel Methods for the Assessment of Miscibility of Amorphous Drug-Polymer Dispersions. *J. Pharm. Sci.* **2009**, *98* (9), 3373–3386.

(24) Moore, M. D.; Shi, Z. Q.; Wildfong, P. L. D. Structural Interpretation in Composite Systems Using Powder X-ray Diffraction: Applications of Error Propagation to the Pair Distribution Function. *Pharm. Res.* **2010**, *27* (12), 2624–2632.

(25) Markovich, R. J.; Evans, C. A.; Coscolluela, C. B.; Zibas, S. A.; Rosen, J. Spectroscopic identification of an amorphous-to-crystalline drug transition in a solid dispersion SCH 48461 capsule formulation. *J. Pharm. Biomed. Anal.* **1997**, *16* (4), 661–673.

(26) Tobyn, M.; Brown, J.; Dennis, A. B.; Fakes, M.; Gao, Q.; Gamble, J.; Khimyak, Y. Z.; McGeorge, G.; Patel, C.; Sinclair, W.; Timmins, P.; Yin, S. Amorphous Drug-PVP Dispersions: Application of Theoretical, Thermal and Spectroscopic Analytical Techniques to the Study of a Molecule With Intermolecular Bonds in Both the Crystalline and Pure Amorphous State. *J. Pharm. Sci.* **2009**, *98* (9), 3456–3468.

(27) Malaj, L.; Censi, R.; Mozzicafreddo, M.; Pellegrino, L.; Angeletti, M.; Gobetto, R.; Di Martino, P. Influence of relative humidity on the interaction between different aryl propionic acid derivatives and poly-(vinylpyrrolydone) K30: Evaluation of the effect on drug bioavailability. *Int. J. Pharm.* **2010**, *398* (1−2), 61–72.

(28) Pham, T. N.; Watson, S. A.; Edwards, A. J.; Chavda, M.; Clawson, J. S.; Strohmeier, M.; Vogt, F. G. Analysis of Amorphous Solid Dispersions Using 2D Solid-State NMR and H-1 T-1 Relaxation Measurements. *Mol. Pharmaceutics* **2010**, *7* (5), 1667–1691.

(29) Vogt, F. G.; Clawson, J. S.; Strohmeier, M.; Edwards, A. J.; Pham, T. N.; Watson, S. A. Solid-State NMR Analysis of Organic Cocrystals and Complexes. *Cryst. Growth Des.* **2009**, *9* (2), 921–937.

(30) Gladden, L. F. Nuclear magnetic resonance in chemical engineering: Principles and applications. *Chem. Eng. Sci.* **1994**, *49* (20), 3339–3408.

(31) Blümich, B. *NMR Imaging of Materials*; Oxford Univ. Press: New York, 2000.

(32) Bowtell, R.; Sharp, J. C.; Peters, A.; Mansfield, P.; Rajabi-Siahboomi, A. R.; Davies, M. C.; Melia, C. D. NMR microscopy of hydrating hydrophilic matrix pharmaceutical tablets. *Magn. Reson. Imaging* **1994**, *12* (2), 361.

(33) Rajabi-Siahboomi, A. R.; Bowtell, R. W.; Mansfield, P.; Henderson, A.; Davies, M. C.; Melia, C. D. Structure and behaviour in hydrophilic matrix sustained release dosage forms: 2. NMR-imaging studies of dimensional changes in the gel layer and core of HPMC tablets undergoing hydration. *J. Controlled Release* **1994**, *31* (2), 121.

(34) Fahie, B. J.; Nangia, A.; Chopra, S. K.; Fyfe, C. A.; Grondey, H.; Blazek, A. Use of NMR imaging in the optimization of a compression-coated regulated release system. *J. Controlled Release* **1998**, *51* (2−3), 179–184.

(35) Fyfe, C. A.; Blazek, A. I. Investigation of hydrogel formation from hydroxypropylmethylcellulose (HPMC) by NMR spectroscopy and NMR imaging techniques. *Macromolecules* **1997**, *30* (20), 6230–6237.

(36) Harding, S.; Baumann, H.; Gren, T.; Seo, A. NMR microscopy of the uptake, distribution and mobility of dissolution media in small, sub-millimetre drug delivery systems. *J. Controlled Release* **2000**, *66* (1), 81–99.

(37) Malveau, C.; Baille, W. E.; Zhu, X. X.; Marchessault, R. H. NMR imaging of high-amylose starch tablets. 2. Effect of tablet size. *Biomacromolecules* **2002**, *3* (6), 1249–1254.

(38) Richardson, J. C.; Bowtell, R. W.; Mader, K.; Melia, C. D. Pharmaceutical applications of magnetic resonance imaging (MRI). *Adv. Drug Delivery Rev.* **2005**, *57* (8), 1191.

(39) Therien-Aubin, H.; Baille, W. E.; Zhu, X. X.; Marchessault, R. H. Imaging of high-amylose starch tablets. 3. Initial diffusion and temperature effects. *Biomacromolecules* **2005**, *6* (6), 3367–3372.

(40) Tritt-Goc, J.; Kowalczuk, J. Spatially resolved solvent interaction with glassy HPMC polymers studied by magnetic resonance microscopy. *Solid State Nucl. Magn. Reson.* **2005**, *28* (2−4), 250.

(41) Tritt-Goc, J.; Pislewski, N. Magnetic resonance imaging study of the swelling kinetics of hydroxypropylmethylcellulose (HPMC) in water. *J. Controlled Release* **2002**, *80* (1−3), 79–86.

(42) Broadbent, A. L.; Fell, R. J.; Codd, S. L.; Lightley, K. A.; Konagurthu, S.; Koehler-King, D. G.; Seymour, J. D. Magnetic resonance imaging and relaxometry to study water transport mechanisms in a commercially available gastrointestinal therapeutic system (GITS) tablet. *Int. J. Pharm.* **2010**, *397* (1−2), 27–35.

(43) Chen, Y. Y.; Hughes, L. P.; Gladden, L. F.; Mantle, M. D. Quantitative ultra-fast MRI of HPMC swelling and dissolution. *J. Pharm. Sci.* **2010**, *99* (8), 3462–3472.

(44) Laity, P. R.; Mantle, M. D.; Gladden, L. F.; Cameron, R. E. Magnetic resonance imaging and X-ray microtomography studies of a gel-forming tablet formulation. *Eur. J. Pharm. Biopharm.* **2010**, *74* (1), 109–119.

(45) Mikac, U.; Sepe, A.; Kristl, J.; Baumgartner, S. A new approach combining different MRI methods to provide detailed view on swelling dynamics of xanthan tablets influencing drug release at different pH and ionic strength. *J. Controlled Release* **2010**, *145* (3), 247–256.

(46) Nott, K. P. Magnetic resonance imaging of tablet dissolution. *Eur. J. Pharm. Biopharm.* **2010**, *74* (1), 78–83.

(47) Dahlberg, C.; Millqvist-Fureby, A.; Schuleit, M.; Furó, I. Relationships between solid dispersion preparation process, particle size and drug release - an NMR and NMR microimaging study. *Eur. J. Pharm. Biopharm.* **2010**, *76* (2), 311–319.

(48) Dahlberg, C.; Fureby, A.; Schuleit, M.; Dvinskikh, S. V.; Furó, I. Polymer mobilization and drug release during tablet swelling. A ^{1}H NMR and NMR microimaging study. *J. Controlled Release* **2007**, *122* (2), 199–205.

(49) Emid, S.; Creyghton, J. H. N. High resolution NMR imaging in solids. *Physica B+C* **1985**, *128* (1), 81–83.

(50) Gravina, S.; Cory, D. G. Sensitivity and resolution of constant-time imaging. *J. Magn. Reson., Ser. B* **1994**, *104* (1), 53–61.

(51) Hyde, T. M.; Gladden, L. F. Simultaneous measurement of water and polymer concentration profiles during swelling of poly(ethylene oxide) using magnetic resonance imaging. *Polymer* **1998**, *39* (4), 811.

(52) Beyea, S. D.; Balcom, B. J.; Prado, P. J.; Cross, A. R.; Kennedy, C. B.; Armstrong, R. L.; Bremner, T. W. Relaxation time mapping of shortT_2* nuclei with single-point imaging (SPI) methods. *J. Magn. Reson.* **1998**, *135* (1), 156–164.

(53) Aso, Y.; Yoshioka, S.; Miyazaki, T.; Kawanishi, T. Feasibility of ^{19}F-NMR for assessing the molecular mobility of flufenamic acid in solid dispersions. *Chem. Pharm. Bull.* **2009**, *57* (1), 61–64.

(54) Sternal, R.; Nugara, N. Flutamide. *Anal. Profiles Drug Subst. Excipients* **2001**, *27*, 115–157.

(55) Silvestri, R. L.; Koenig, J. L. A T_1 spin-lattice relaxation and a cross-polarization dynamics study of the molecular motions of a side-chain liquid-crystalline polymer. *Macromolecules* **1992**, *25* (9), 2341–2350.

(56) Gao, P. Characterization of three crystalline forms (VIII, XI, and XII) and the amorphous form (V) of delavirdine mesylate using ^{13}C CP/MAS NMR. *Pharm. Res.* **1998**, *15* (9), 1425–1433.

(57) Aso, Y.; Yoshioka, S.; Kojima, S. Relationship between the crystallization rates of amorphous nifedipine, phenobarbital, and flopropione, and their molecular mobility as measured by their enthalpy relaxation and ^{1}H NMR relaxation times. *J. Pharm. Sci.* **2000**, *89* (3), 408–416.

(58) Aso, Y.; Yoshioka, S.; Kojima, S. Explanation of the crystallization rate of amorphous nifedipine and phenobarbital from their molecular mobility as measured by ^{13}C nuclear magnetic resonance relaxation time and the relaxation time obtained from the heating rate dependence of the glass transition temperature. *J. Pharm. Sci.* **2001**, *90* (6), 798–806.

(59) Murakami, M.; Ishida, H.; Kaji, H.; Horii, F. Solid-state C-13 NMR studies of the structure and chain conformation of thermotropic liquid crystalline polyether crystallized from the liquid crystalline glassy phase. *Polym. J.* **2004**, *36* (5), 403–412.

(60) Masuda, K.; Tabata, S.; Sakata, Y.; Hayase, T.; Yonemochi, E.; Terada, K. Comparison of molecular mobility in the glassy state between amorphous indomethacin and salicin based on spin-lattice relaxation times. *Pharm. Res.* **2005**, *22* (5), 797–805.

(61) Apperley, D. C.; Forster, A. H.; Fournier, R.; Harris, R. K.; Hodgkinson, P.; Lancaster, R. W.; Rades, T. Characterisation of indomethacin and nifedipine using variable-temperature solid-state NMR. *Magn. Reson. Chem.* **2005**, *43* (11), 881–892.

(62) Lubach, J. W.; Xu, D. W.; Segmuller, B. E.; Munson, E. J. Investigation of the effects of pharmaceutical processing upon solid-state NMR relaxation times and implications to solid-state formulation stability. *J. Pharm. Sci.* **2007**, *96* (4), 777–787.

(63) Adam-Berret, M.; Riaublanc, A.; Rondeau-Mouro, C.; Mariette, F. Effects of crystal growth and polymorphism of triacylglycerols on NMR relaxation parameters. 1. Evidence of a relationship between crystal size and spin-lattice relaxation time. *Cryst. Growth Des.* **2009**, *9* (10), 4273–4280.

(64) Ulrich, A. S. Solid state ^{19}F NMR methods for studying biomembranes. *Prog. Nucl. Magn. Reson. Spectrosc.* **2005**, *46* (1), 1–21.

(65) Emid, S.; Baarda, R. J.; Smidt, J.; Wind, R. A. Influence of symmetry-restricted spin diffusion on spin-lattice relaxation of molecular groups in solids. *Physica B+C* **1978**, *93* (3), 327–343.

(66) Torchia, D. A.; Szabo, A. Spin-lattice relaxation in solids. *J. Magn. Reson.* **1982**, *49* (1), 107–121.

(67) Abragam, A. *Principles of Nuclear Magnetism*; Oxford Univ. Press: Oxford, 1961.

(68) Cowan, B. *Nuclear Magnetic Resonance and Relaxation*; Cambridge Univ. Press: 1997.

(69) Wang, S. C.; Tsa, H. K. Ion migration through a polymer solution: Microviscosity. *Macromolecules* **2003**, *36* (24), 9128–9134.

(70) Cheong, L. W. S.; Heng, P. W. S.; Wong, L. F. Relationship between polymer viscosity and drug release from a matrix system. *Pharm. Res.* **1992**, *9* (11), 1510–1514.

(71) ShinEtsu. *Pharmacoat*; Cellulose and pharmaceutical excipient department: Tokyo, 2004.

(72) Powles, J. G.; Mansfield, P. Double-pulse nuclear-resonance transients in solids. *Phys. Lett.* **1962**, *2*, 56–59.

(73) Beckmann, P. A.; Rosenberg, J.; Nordstrom, K.; Mallory, C. W.; Mallory, F. B. CF3 rotation in 3-(trifluoromethyl)phenanthrene: Solid state F-19 and H-1 NMR relaxation and Bloch-Wangsness-Redfield theory. *J. Phys. Chem. A* **2006**, *110* (11), 3947–3953.

(74) Siepe, S.; Herrmann, W.; Borchert, H. H.; Lueckel, B.; Kramer, A.; Ries, A.; Gurny, R. Microenvironmental pH and microviscosity inside pH-controlled matrix tablets: An EPR imaging study. *J. Controlled Release* **2006**, *112* (1), 72–78.

(75) Kowalewski, J.; Mäler, L. *Nuclear Spin Relaxation in Liquids*; CRC Press: Boca Raton, 2006.

(76) Wennerström, H.; Lindblom, G.; Lindman, B. Theoretical aspects on the NMR of quadrupolar ionic nuclei in micellar solutions and amphiphilic liquid crystals. *Chem. Scr.* **1974**, *6*, 97–103.

(77) Wennerström, H.; Lindman, B.; Söderman, O.; Drakenberg, T.; Rosenholm, J. B. ^{13}C Magnetic Relaxation in Micellar Solutions. Influence of Aggregate Motion on T_1. *J. Am. Chem. Soc.* **1979**, *101*, 6860–6864.

(78) Lipari, G.; Szabo, A. Model-free approach to the interpretation of nuclear magnetic resonance relaxation in macromolecules. 1. Theory and range of validity. *J. Am. Chem. Soc.* **1982**, *17*, 4546–4559.

(79) Matson, G. B. Methyl NMR relaxation due to dipolar interactions. *J. Chem. Phys.* **1975**, *65*, 4147–4154.

(80) Werbelow, L. G.; Marshall, A. G. Internal rotation and non-exponential methyl nuclear relaxation for macromolecules. *J. Magn. Reson.* **1973**, *11* (2), 299–313.

(81) Katzhendler, I.; Mäder, K.; Friedman, M. Structure and hydration properties of hydroxypropyl methylcellulose matrices containing naproxen and naproxen sodium. *Int. J. Pharm.* **2000**, *200* (2), 161–179.

(82) Dahlberg, C.; Millqvist-Fureby, A.; Schuleit, M.; Furó, I. Polymer-drug interactions and wetting of solid dispersions. *Eur. J. Pharm. Sci.* **2010**, *39* (1−3), 125–133.

(83) Penn, R. L.; Banfield, J. F. Formation of rutile nuclei at anatase {112} twin interfaces and the phase transformation mechanism in nanocrystalline titania. *Am. Mineral.* **1999**, *84* (5−6), 871–876.

(84) Zhang, H. Z.; Banfield, J. F. Phase transformation of nanocrystalline anatase-to-rutile via combined interface and surface nucleation. *J. Mater. Res.* **2000**, *15* (2), 437–448.

(85) Zhang, H. Z.; Banfield, J. F. Polymorphic transformations and particle coarsening in nanocrystalline titania ceramic powders and membranes. *J. Phys. Chem. C* **2007**, *111* (18), 6621–6629.

(86) Colfen, H.; Qi, L. M. A systematic examination of the morphogenesis of calcium carbonate in the presence of a double-hydrophilic block copolymer. *Chem.—Eur. J.* **2001**, *7* (1), 106–116.

(87) Judat, B.; Kind, M. Morphology and internal structure of barium sulfate - derivation of a new growth mechanism. *J. Colloid Interface Sci.* **2004**, *269* (2), 341–353.

(88) Rieger, J.; Frechen, T.; Cox, G.; Heckmann, W.; Schmidt, C.; Thieme, J. Precursor structures in the crystallization/precipitation processes of $CaCO_3$ and control of particle formation by polyelectrolytes. *Faraday Discuss.* **2007**, *136*, 265–277.